Discovery of superconductivity in technetium-borides at moderate pressures

Xiangru Tao,[1] Aiqin Yang,[1] Yundi Quan,[1] Biao Wan,[2] Shuxiang Yang,[3] and Peng Zhang[1]

[1]*MOE Key Laboratory for Non-equilibrium Synthesis and Modulation of Condensed Matter, Shaanxi Province Key Laboratory of Advanced Functional Materials and Mesoscopic Physics, School of Physics, Xi'an Jiaotong University, 710049, Xi'an, Shaanxi, P.R.China*
[2]*Key Laboratory of Material Physics of Ministry of Education, School of Physics and Microelectronics, Zhengzhou University, Zhengzhou 450052, Henan, P.R.China*
[3]*Zhejiang laboratory, Hangzhou, Zhejiang, P.R.China*

I. METHODS

A. Particle swarm optimization algorithm

We adopt the particle swarm optimization (PSO) based CALYPSO (Crystal structure AnaLYsis by Particle Swarm Optimization) package [1] in searching for new structures. As a stochastic algorithm, in each iteration of PSO all potential solutions are treated as swarm of particles with certain velocities in the search space of the given problem. The current position and the trajectory of particles in swarm will be stored and broadcast, so as to determine the next moves through the search space. After each iteration, the swarm gradually approach the optimum of the objective function, which is the total-energy in case of structure searches. Both global and local PSO algorithms have been implemented in CALYPSO package, which enables the advantages of efficient convergence and capability in dealing with complex systems.

B. Structure search

The searches for compounds of Tc_xB_y stoichiometry were done at 0, 90 and 180 GPa. In each generation, 60% derived structures of the lowest formation enthalpy are preserved for the next iteration, and 40% new structures are randomly generated. At each pressure above 6700 structures have been generated and totally more than 25000 structures have been derived. The projector augmented-wave [2, 3] density functional theory (PAW-DFT) as implemented in Vienna Ab-initio Simulation Package (VASP) [4–6] and the Perdew-Burke-Ernzerhof generalized gradient approximation (GGA-PBE) [7] exchange-correlation functional are used. Valence electron configurations in PAW potential is Tc-$4p^6 4d^5 5s^2$ and B-$2s^2 2p^1$. Plane-wave energy cutoff of 350 eV, Γ-centered k-point meshes with a resolution of $2\pi\times$ 0.05 $Å^{-1}$ for Brillouin zone sampling, energy and force convergence criteria of $1 \times e^{-9}$ eV and 0.03 eV/Å respectively, are adopted for total energy calculations and structure relaxations. In derivation of composition-pressure phase diagram, we use higher precision with plane-wave energy cutoff of 500 eV, Γ-centered k-point meshes resolution of 2π × 0.03 $Å^{-1}$, energy and force convergence criteria of $1 \times e^{-9}$ eV and 0.01 eV/Å.

C. Electron-phonon calculations

The electronic structures and the phonon properties are calculated using QUANTUM-ESPRESSO (QE) package [8]. The plane-wave kinetic-energy cutoff and the charge density energy cutoff are 100 Ry and 400 Ry, respectively. Optimized norm-conversing pseudopotential with valence electron configurations of Tc-$4p^6 4d^5 5s^2$ and B-$2s^2 2p^1$ and Methfessel-Paxton smearing [9] width of 0.02 Ry are used. The setup of k-grids and q-grids in electron-phonon calculations is presented in Table I. The dynamic matrix and the electron-phonon coupling (EPC) constant λ are calculated using the density-functional perturbation theory [10]. Superconducting transition temperature is estimated following the Allen-Dynes modified McMillan equation [11],

$$T_c = \frac{\omega_{\log}}{1.2} \exp\left[-\frac{1.04(1+\lambda)}{\lambda - \mu^*(1+0.62\lambda)}\right], \quad (1)$$

in which λ is the average EPC parameter, $\omega_{\log}$ is the logarithmic average frequency, and the Coulomb pseudopotential [12] $\mu^* = 0.12$. The dependence of superconducting transition temperatures T_c of five thermodynamically metastable technetium-borides on Coulomb pseudopotential μ^* is presented in Fig. 1.

TABLE I: Setting of k-points and q-points in calculations of superconducting temperatures by Quantum Espresso.

Formula	Space group	P (GPa)	Kmesh1	Kmesh2	Qmesh
TcB_2	P6/mmm	20	60×60×60	15×15×15	5×5×5
TcB	$P6_3/mmc$	0	96×96×48	16×16×8	8×8×4
Tc_2B	I4/mcm	0	45×45×45	9×9×9	3×3×3
Tc_3B	P4/mmm	0	60×60×36	15×15×9	5×5×3
TcB	Cmcm	30	27×9×27	9×3×9	3×1×3

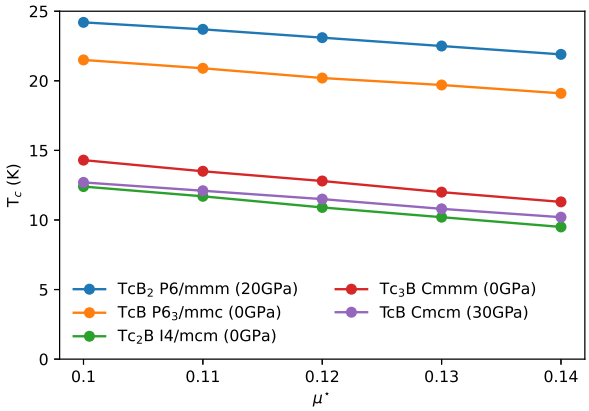

FIG. 1: The superconducting transition temperatures T_c of five thermodynamically metastable technetium-borides as a function of the Coulomb pseudopotential μ^*.

II. ELASTIC CONSTANT

TABLE II: The calculated elastic constants C_{ij} (GPa), bulk modulus B (GPa), shear modulus S (GPa), Young's modulus Y (GPa), Poisson's ratio V, and Vickers hardness H_v of superconducting technetium-borides at their lowest dynamically stable pressures.

Formula	Space Group	B	Y	S	$H_{v,chen}$	$H_{v,Tian}$	C_{11}	C_{12}	C_{13}	C_{21}	C_{22}	C_{23}	C_{31}	C_{32}	C_{33}	C_{44}	C_{55}	C_{66}
TcB2 (20GPa)	P6/mmm	362.0	399.8	151.9	10.6	12.0	685	213	220	213	685	220	220	220	589	85	85	236
TcB (0GPa)	$P6_3/mmc$	292.6	222.0	80.8	2.8	4.8	394	231	230	231	394	230	230	230	475	69	69	82
Tc2B (0GPa)	I4/mmm	318.8	381.1	146.5	11.8	13.0	547	171	227	171	547	227	227	227	526	123	123	164
Tc3B (0GPa)	P4/mmm	311.7	351.1	133.8	10.0	11.3	449	229	241	229	449	241	241	241	490	128	128	202
TcB (30GPa)	Cmcm	407.9	459.9	175.3	12.2	13.7	637	321	294	321	498	342	294	342	641	170	292	193

According to Mouhat's work[13], all five superconductors are mechanically stable. For Tetragonal I structures, I4/mmm-Tc2B and P4/mmm-Tc3B, following criteria are satisfied: (i) $C_{11} > |C_{12}|$. (ii) $2C_{13}^2 < C_{33}(C_{11} + C_{12})$. (iii) $C_{44} > 0$. (iv) $C_{66} > 0$.

For Orthorhombic crystal Cmcm-TcB , Elastic stability criteria are: (i) $C_{11} > > 0$. (ii) $C_{11}{\times}C_{22} > C_{12}^2$. (iii) $C_{11}{\times}C_{22}{\times}C_{33} + 2C_{12}{\times}C_{13}{\times}C_{23} - C_{11}{\times}C_{23}^2 - C_{22}{\times}C_{13}^2 - C_{33}{\times}C_{12}^2 > 0$. (iv) $2C_{13}^2 < C_{33}(C_{11} + C_{12})$. (vi) $C_{44} > 0$. (vii) $C_{55} > 0$. (viii) $C_{66} > 0$.

For Hexagonal crystal P6/mmm-TcB2 and $P6_3/mmc$-TcB , Elastic stability criteria are: (i) $C_{11} > |C_{12}|$. (ii) $2C_{13}^2 < C_{33}(C_{11} + C_{12})$. (iii) $C_{44} > 0$.

III. BAND STRUCTURE, PARTIAL DENSITY OF STATES AND FERMI SURFACE

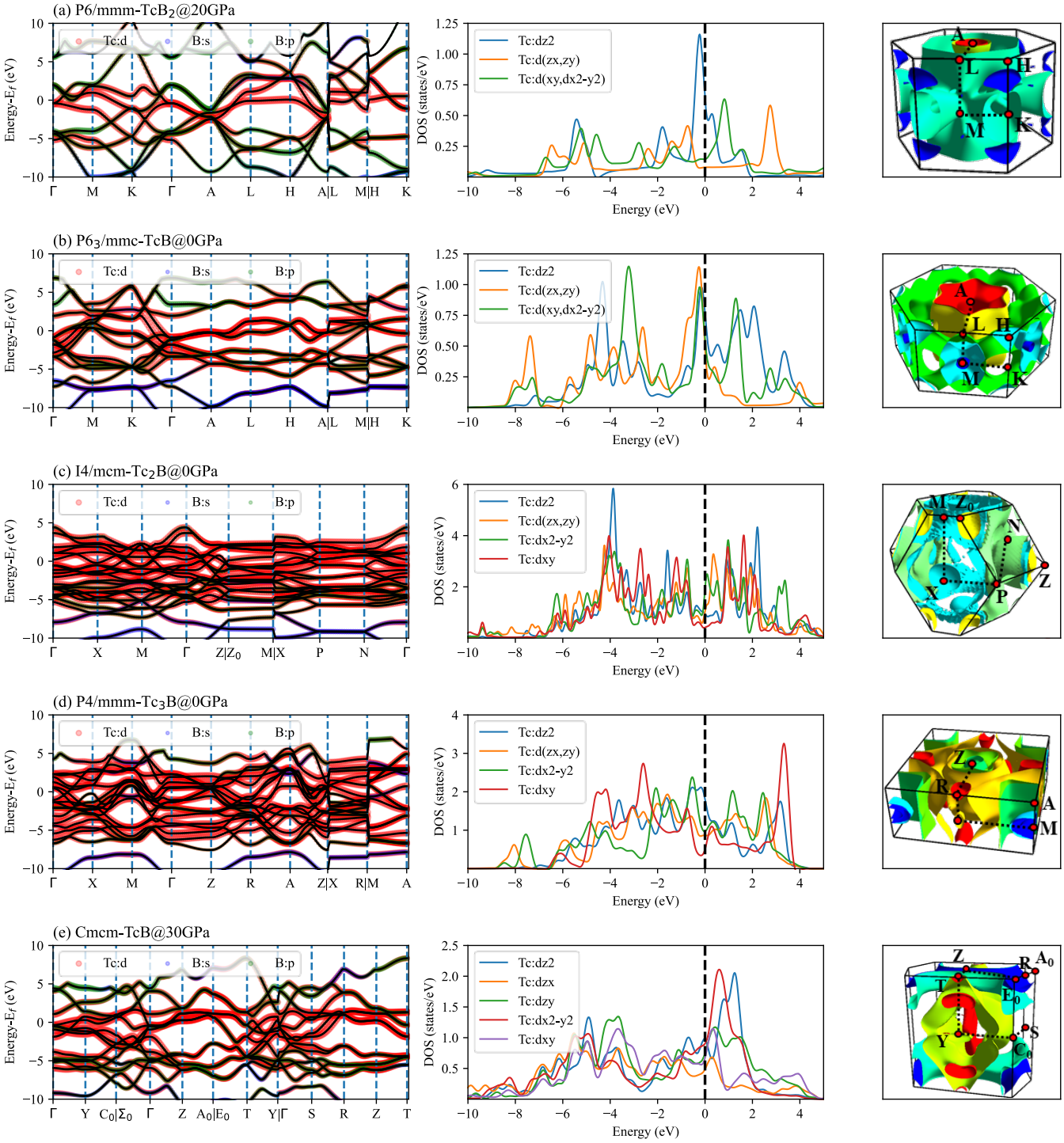

FIG. 2: The fatband, the Tc-4d partial density of states, and the Fermi surfaces of superconducting technetium-borides at their lowest dynamically stable pressures.

IV. CRYSTAL STRUCTURES AND XRD

TABLE III: Crystal structure information of superconducting technetium-borides at their minimum dynamically stable pressures.

Formula	Space Group	P (GPa)	Lattice	Atom	Wyckoff Site	x	y	z
Tc_2B	I4/mcm	0	a,b=5.45112, c=4.58875 α,β,γ=90.00	Tc	8h	0.165870	0.334130	0.500000
				B	4a	0.000000	0.000000	0.250000
Tc_3B	P4/mmm	0	a,b=2.73625, c=6.53966 α,β,γ=90.00	Tc	2h	0.500000	0.500000	0.299594
				Tc	1a	0.000000	0.000000	0.000000
				B	1b	0.000000	0.000000	0.500000
TcB_2	P6/mmm	20	a,b=2.90764, c=3.33220 α,β=90.00, γ=120.00	Tc	1a	0.000000	0.000000	0.000000
				B	2d	0.333333	0.666667	0.500000
TcB	$P6_3/mmc$	0	a,b=2.98762, c=5.39824 α,β=90.00, γ=120.00	Tc	2d	0.333333	0.666667	0.750000
				B	2a	0.000000	0.000000	0.000000
	Cmcm	30	a=2.96052, b=8.44992, c=2.93710 α,β,γ=90.00	Tc	4c	0.500000	0.359965	0.250000
				B	4c	0.500000	0.062865	0.250000

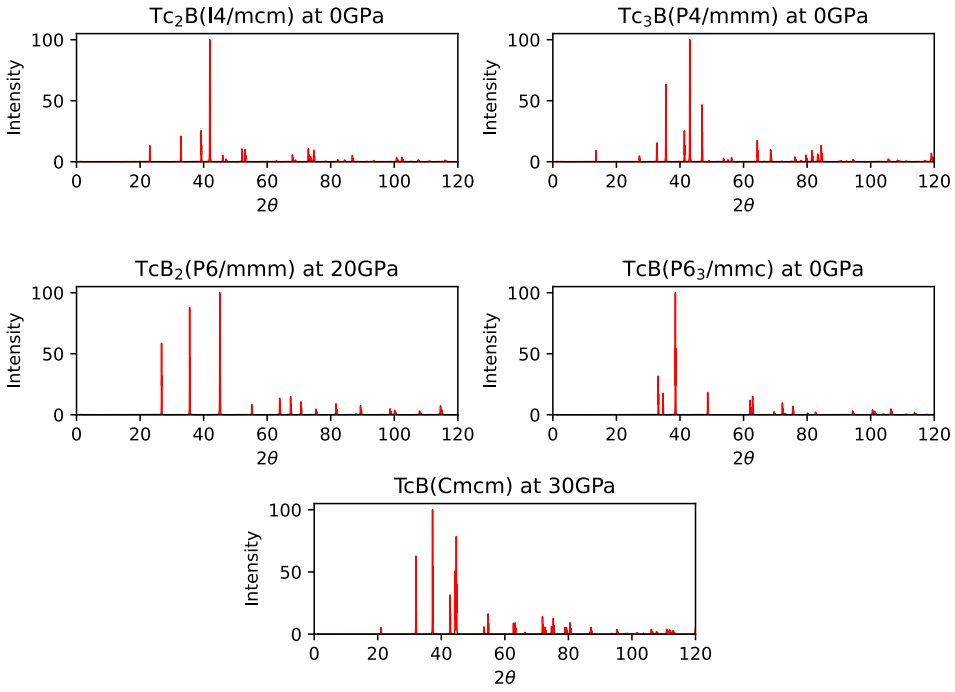

FIG. 3: The X-ray diffraction pattern of superconducting technetium-borides at their minimum dynamically stable pressures.

TABLE IV: Crystal structure information of thermodynamically stable technetium-borides on the convex hull at minimum pressures of their stable presence.

Formula	Space Group	P(GPa)	Lattice	Atom	Wyckoff Site	x	y	z
Tc_3B	Cmcm	0	a=2.91275, b=9.23801, c=7.23020 α,β,γ=90.00	Tc	8f	0.000000	0.134864	0.061586
				Tc	4c	0.000000	0.424640	0.250000
				B	4c	0.000000	0.256035	0.750000
Tc_7B_3	$P6_3mc$	0	a=7.49018, b=7.49018, c=4.84714 α,β=90.00, γ=120.00	Tc	6c	0.091444	0.545722	0.548556
				Tc	6c	0.123690	0.247380	0.254361
				Tc	2b	0.333333	0.666667	0.083239
				B	6c	0.189486	0.378972	0.840006
Tc_2B	C2/m	30	a=9.08524, b=2.82434, c=6.18676 γ,α=90.00, β=127.14	Tc	4i	0.088603	0.500000	0.371883
				Tc	4i	0.664062	0.500000	0.082952
				B	4i	0.114749	0.000000	0.669473
	Fddd	70	a=4.27497, b=7.44655, c=14.70511 α,β,γ=90.00	Tc	16g	0.500000	0.000000	0.917324
				Tc	16f	0.000000	0.168933	0.000000
				B	16g	0.500000	0.000000	0.624551
TcB	$P2_1$	30	a=4.29808, b=5.86289, c=5.81790 γ,α=90.00, β=90.03	Tc	2a	0.132513	0.809631	0.259501
				Tc	2a	0.137240	0.826455	0.739666
				Tc	2a	0.361956	0.176998	0.016808
				Tc	2a	0.365246	0.176744	0.481445
				B	2a	0.140431	0.529324	0.997154
				B	2a	0.148684	0.525550	0.503919
				B	2a	0.354157	0.458645	0.751918
				B	2a	0.366385	0.475243	0.248344
	$Pmn2_1$	70	a=5.63663, b=4.20428, c=5.72358 α,β,γ=90.00	Tc	4b	0.237207	0.364271	0.676269
				Tc	2a	0.000000	0.132960	0.312490
				Tc	2a	0.000000	0.863248	0.824731
				B	4b	0.247299	0.856982	0.527743
				B	2a	0.000000	0.364130	0.973326
				B	2a	0.000000	0.644823	0.459989
	Pnma	170	a=5.48366, b=2.67958, c=4.02962 α,β,γ=90.00	Tc	4c	0.177742	0.750000	0.386735
				B	4c	0.030572	0.750000	0.891267
Tc_3B_4	C2/m	160	a=7.29105, b=2.74764, c=5.39301 γ,α=90.00, β=112.93	Tc	4i	0.687754	0.500000	0.154769
				Tc	2c	0.000000	0.000000	0.500000
				B	4i	0.028510	0.500000	0.843043
				B	4i	0.190255	0.500000	0.433562
TcB_2	$P6_3/mmc$	0	a,b=2.89412, c=7.45850 α,β=90.00, γ=120.00	Tc	2d	0.333333	0.666667	0.750000
				B	4f	0.333333	0.666667	0.452349
	$I4_1/amd$	180	a,b=2.77872, c=9.76920 α,β,γ=90.00	Tc	4b	0.500000	0.500000	0.000000
				B	8e	0.000000	0.000000	0.085042
TcB_3	$P\bar{6}m2$	10	a,b=2.87002, c=4.53652 α,β=90.00, γ=120.00	Tc	1f	0.666667	0.333333	0.500000
				B	2h	0.333333	0.666667	0.180736
				B	1e	0.666667	0.333333	0.000000
TcB_4	$P6_3/mmc$	40	a,b=2.79644, c=10.51697 α,β=90.00, γ=120.00	Tc	2d	0.333333	0.666667	0.750000
				B	4f	0.333333	0.666667	0.384967
				B	4f	0.333333	0.666667	0.958044

[1] Y. Wang, J. Lv, L. Zhu, and Y. Ma, Comput. Phys. Commun. **183**, 2063 (2012), ISSN 0010-4655.
[2] P. E. Blöchl, Phys. Rev. B **50**, 17953 (1994).
[3] G. Kresse and D. Joubert, Phys. Rev. B **59**, 1758 (1999).
[4] G. Kresse and J. Hafner, Phys. Rev. B **47**, 558 (1993).

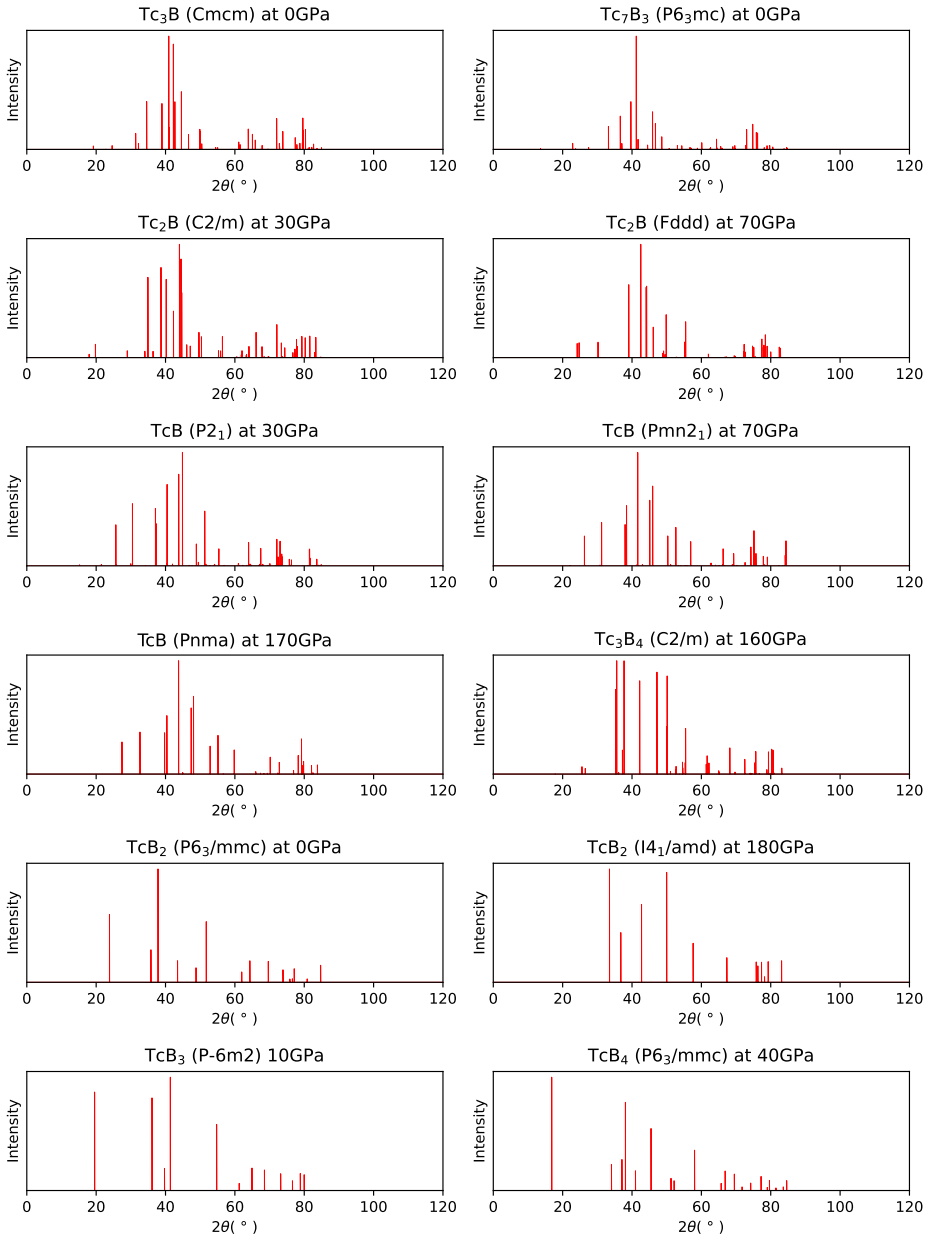

FIG. 4: The X-ray diffraction pattern of thermodynamically stable technetium-borides on the convex hull at the minimum pressures of their stable presence.

[5] G. Kresse and J. Hafner, Phys. Rev. B **49**, 14251 (1994).
[6] G. Kresse and J. Furthmüller, Phys. Rev. B **54**, 11169 (1996).
[7] J. P. Perdew, K. Burke, and M. Ernzerhof, Phys. Rev. Lett. **77**, 3865 (1996), URL https://link.aps.org/doi/10.1103/PhysRevLett.77.3865.
[8] P. Giannozzi, S. Baroni, N. Bonini, M. Calandra, R. Car, C. Cavazzoni, D. Ceresoli, G. L. Chiarotti, M. Cococcioni, and I. Dabo, J. Phys. Condens. Matter **21**, 395502 (2009), ISSN 0953-8984.
[9] M. Methfessel and A. Paxton, Phys. Rev. B **40**, 3616 (1989).
[10] S. Baroni, S. De Gironcoli, A. Dal Corso, and P. Giannozzi, Rev. Mod. Phys. **73**, 515 (2001).
[11] P. B. Allen and R. C. Dynes, Phys. Rev. B **12**, 905 (1975), URL https://link.aps.org/doi/10.1103/PhysRevB.12.905.
[12] P. Morel and P. W. Anderson, Phys. Rev. **125**, 1263 (1962), URL https://link.aps.org/doi/10.1103/PhysRev.125.1263.
[13] F. Mouhat and F. Coudert, Phys. Rev. B **90**, 224104 (2014), URL https://link.aps.org/doi/10.1103/PhysRevB.90.224104.